Tectonophysics 457 (2008) 1–11

Contents lists available at ScienceDirect

Tectonophysics

journal homepage: www.elsevier.com/locate/tecto

Rollovers in salt tectonics: The inadequacy of the listric fault model

Jean-Pierre Brun, Thomas P.-O. Mauduit *

Géosciences Rennes UMR 6118 CNRS, University Rennes 1, 35042 Rennes cedex, France

ARTICLE INFO

Article history:
Received 21 May 2007
Received in revised form 26 October 2007
Accepted 13 November 2007

Keywords:
Salt tectonics
Growth fault/rollover
Listric fault
Graben
Antithetic versus synthetic rollovers
Passive margin
Extension

ABSTRACT

Rollover anticlines are syn-sedimentary extensional structures, common in salt tectonics, that are classically considered to result from layer bending during hangingwall displacement above a listric normal fault. However, theoretical considerations and seismic images of natural examples put in question the validity of the listric fault model from which rollover growth is steady state, by nature, and controlled by the relative displacement of two blocks.

We used laboratory experiments of gravity driven deformation of brittle–ductile models simulating salt tectonics processes to study in which circumstances rollovers are obtained both in time and space. It is argued that rollover growth is a nonsteady process that results from a mechanical instability whose critical lifetime can be divided in three characteristic stages: birth, growth, and decay.

In kinematic terms, the development of a synthetic or antithetic rollover requires a three-block system: an upslope block and a downslope block that move downslope and that separate from each other on top of an extending décollement layer lying above a basement block. Synthetic and antithetic rollovers developed with upward concave shapes whatever the sense of shear in the salt layer and can pass laterally to each other without transform fault. This points out that the concave shape of a rollover base is not an argument in favour of listric faulting. The concave shape simply results from the connection between a steeply dipping normal fault and a flat lying or gently dipping décollement.

1. Introduction

Rollover anticlines are syn-sedimentary extensional structures that commonly occur in basins undergoing gravity driven deformation over a salt or shale décollement layer (Fig. 1) (e.g. Cloos, 1968; Edwards, 1976; Rider, 1978; Bally, 1981; Bally et al., 1981; Shelton, 1984; Gibbs, 1985; Nelson, 1991; Kerr and White, 1992; Liro and Coen, 1995; Mohriak et al., 1995; Szatmari et al., 1996; Bhattacharya and Davies, 2001; Imber et al., 2003). Their characteristic geometry is classically interpreted as a direct consequence of layer bending during hangingwall displacement above a listric normal fault (Fig. 2) that continuously transforms a steeply plunging displacement vector at the surface to a nearly horizontal one at depth (Bally et al., 1981; Shelton, 1984). It is generally agreed that the listric shape results from the connection between a newly formed steeply normal fault and a pre-existing low angle décollement layer, where fluid pressure is abnormally high (Bruce, 1973; Price, 1977; Mandl and Crans, 1981; Bradshaw and Zoback, 1988) or which is made of weak materials (Burollet, 1975; Bally et al., 1981; Gibbs, 1983, 1984, 1985; Vendeville and Cobbold, 1987; Vendeville, 1991; Duval et al., 1992; Lundin, 1992). The properties and predictions of this conceptual and theoretical "listric fault model" have been largely explored through numerical modelling (see recent review by Poblet and Bulnes, 2005) and analogue modelling (e.g. Vendeville and Cobbold, 1987; Ellis and McClay, 1988; McClay et al., 1991; McClay, 1995, 1996; Mauduit and Brun, 1998). It is also explicitly or implicitly involved in the various computing procedures proposed to predict normal fault geometries and depth of décollement from the geometry of hangingwall layers (e.g. Davison, 1986; White et al., 1986; Wheeler, 1987; William and Van, 1987; Xiao and Suppe, 1989; Braun et al., 1994; for critical reviews of methods see Dula, 1991; Withjack and Peterson, 1993; Hauge and Gray, 1996; Poblet and Bulnes, 2005).

In seismic images (Fig. 1), a rollover most often corresponds to an asymmetrical anticline in which the thickness of sedimentary layers increases with dip, toward the master fault. The external envelope of the rollover has a bulk upward concave shape made, in its steep part, of a normal fault affecting sedimentary layers (thick lines in sections of Fig. 1) and, in its low dipping part, of a contact between the sedimentary layers of the rollover and a weak layer made of salt or other soft rocks (dotted lines in sections of Fig. 1). The basal weak layer displays important thickness variations and defines a roller below the steeply dipping normal fault (noted R in sections of Fig. 1). The steeply dipping normal fault can reach the surface and even offset the seabed indicating that it is still active (e.g. Fig. 1b). The normal fault can also be sealed by overlying sedimentary layers indicating that it is no more active (e.g. Fig. 1a and c). The outer-arc part of the rollover generally displays series of normal faults dipping either toward (in the youngest part of rollover in Fig. 1a) or parallel to (Fig. 1c) the master normal

* Corresponding author.
E-mail addresses: jean-pierre.brun@univ-rennes1.fr (J.-P. Brun), thomas@mauduit.org (T.P.-O. Mauduit).

0040-1951/$ – see front matter © 2007 Elsevier B.V. All rights reserved.
doi:10.1016/j.tecto.2007.11.038

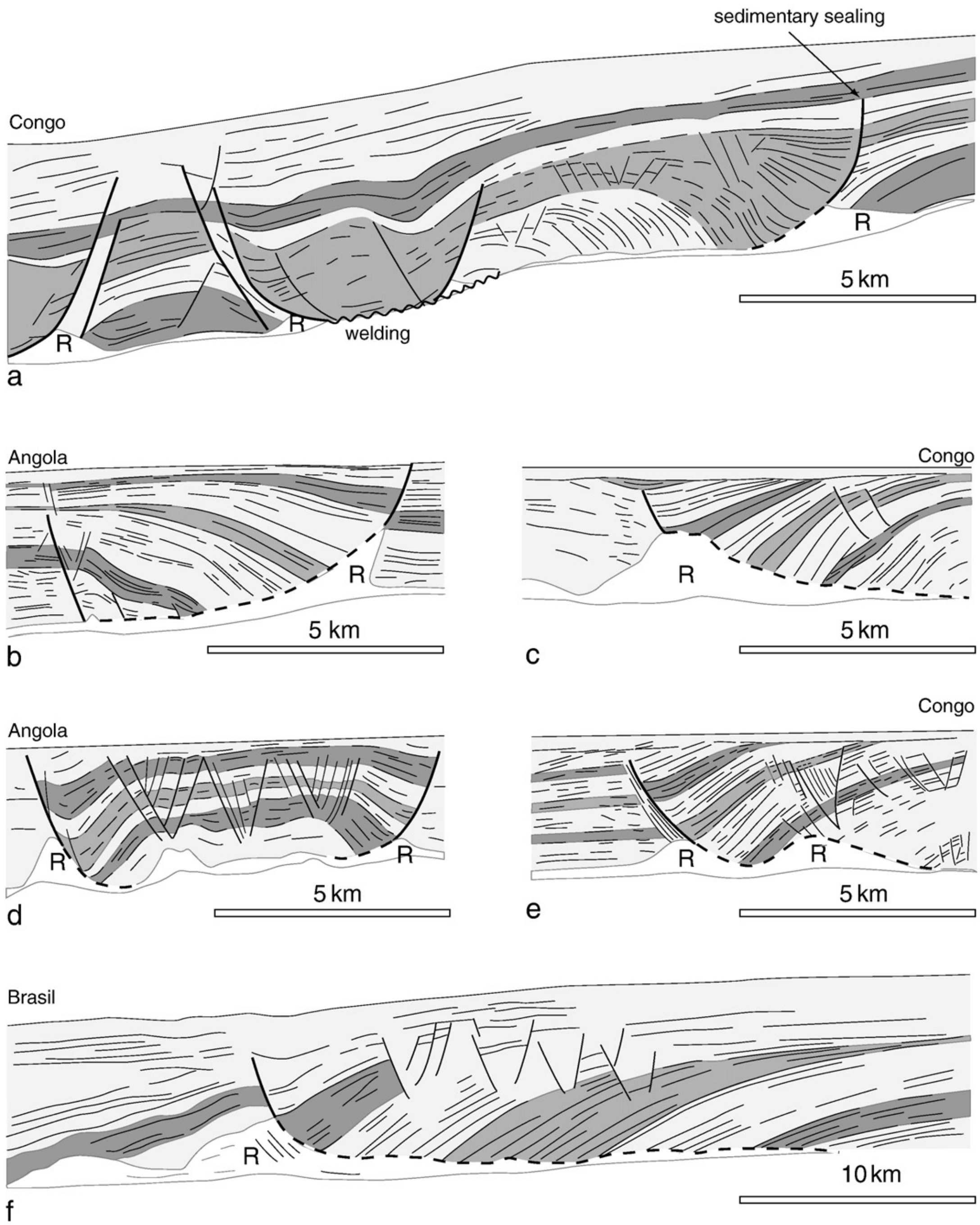

Fig. 1. Examples of rollovers from South Atlantic passive margins. All sections are oriented with the basal salt layer dipping to the right — i.e. toward the oceanic domain. a and b: Synthetic rollovers; c, e and f: antithetic rollovers; d: turtle back-type anticline. Sources of seismic data used for the line drawings: a: Rouby et al. (2002); b: Faure and Chermette (1989), c and e: Mauduit and Brun (1998); d: Mauduit (1998); f: Demercian et al. (1993). R: Salt rollers.

fault. Where faults are conjugate they often define Y-shape patterns that control the development of syn-sedimentary grabens (Fig. 1a, b, d and f), often called keystone or crestal collapse graben. Fault sealing by sedimentary layers indicate faulting sequences with youngest ages toward the master normal fault (Fig. 1a, c, e and f). Finally, rollovers can reach several tens of kilometres in width as exemplified on the Brazilian margin (Demercian et al., 1993).

Rollovers that develop in passive margin-type salt tectonics fall into two kinematic categories according to the sense of dip of the master fault. They are “synthetic” when the fault dips in the same sense than the basal slope (Fig. 1a and b) and “antithetic” when it dips in the opposite sense (Fig. 1c, e and f). Instead of synthetic and antithetic, more geographical terminologies are also used such as “seaward” and “landward” or “regional” and “counter-regional”, respectively. On a number of passive margins, antithetic rollovers are coeval to synthetic ones, on their downslope side (e.g. Gabon margin (Fig. 4, in Seranne et al., 1992), Angolan margin (Fig. 4, in Broucke et al., 2004, and Fig. 2, in Fort et al., 2004a,b)). Antithetic rollovers are also common and well developed in prograding deltas (e.g. Doust and Omatsola, 1990). The narrow association of synthetic and antithetic rollovers with facing normal faults gives turtle back-type structures (Fig. 1d), in which detailed structural and stratigraphic analysis in general reveals that synthetic and antithetic components develop diachronously (Lundin, 1992; Mauduit et al., 1997a).

The basal envelope of rollovers is often irregular in particular in antithetic examples (Fig. 1c, e and f). Small amplitude irregularities

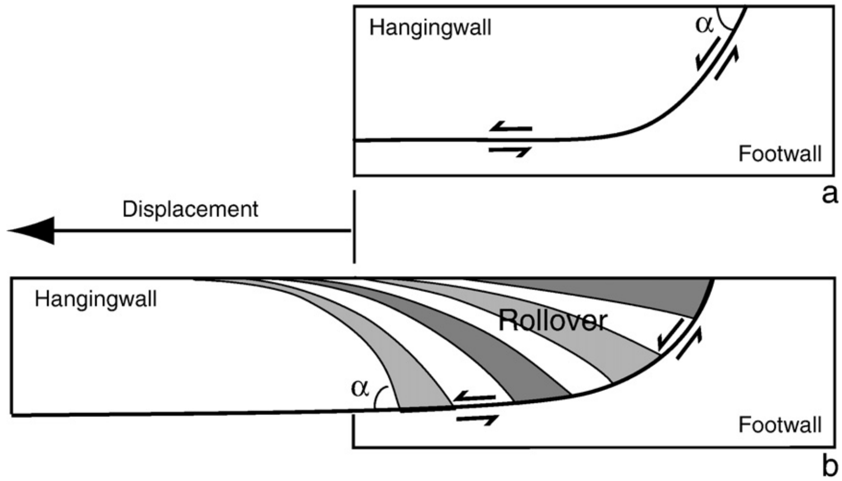

Fig. 2. The classical model of listric fault and rollover.

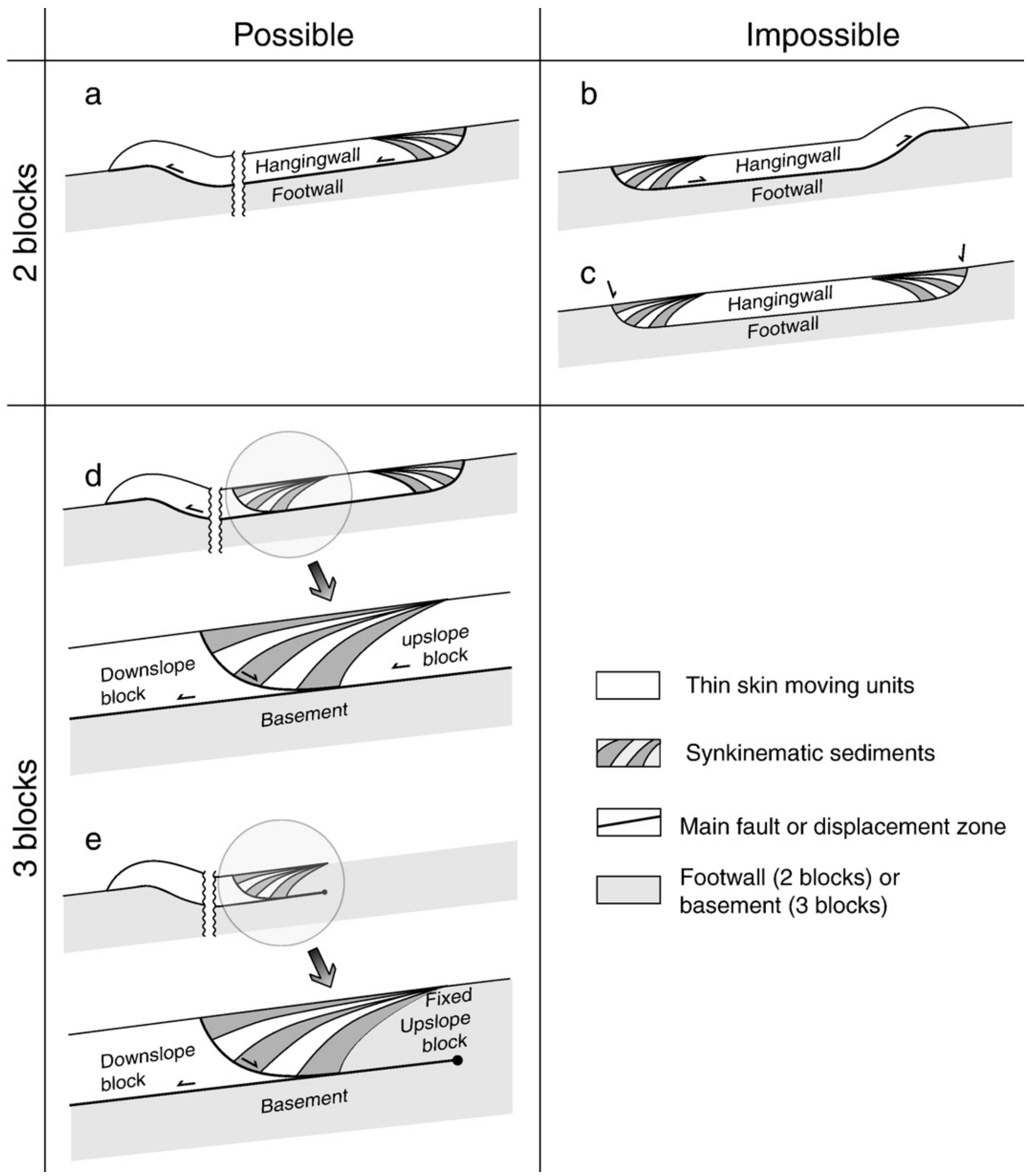

Fig. 3. The accommodation of antithetic rollovers displacements. In the frame of two-block systems, the development of a synthetic rollover can be accommodated by thrusting downslope (a) but the development of an antithetic rollover remains impossible either by thrusting (b) or extension (c). In the frame of three-block systems the development of antithetic rollovers become possible between blocks moving at different rates on top of a basement, with an upslope block mobile (d) or fixed (e). In the later case the upslope block cannot move downslope but is progressively rotated in parallelism with the basement as the downslope block moves.

(e.g. Fig. 1f) could be due to seismic artefacts but larger ones (e.g. Fig. 1c, d, and e) cannot be explained in this way and reflect significant variations in the rollover growth process (Mauduit and Brun, 1998). Such strongly distorted shapes of the rollover envelope are far from the classical listric geometry.

The application of the implicit boundary conditions of the 2-block listric fault model – i.e. an upward concave fault that separates a hangingwall block from a footwall block (Fig. 2) – to the regional setting of synthetic and antithetic rollovers at margin scale leads to obvious kinematical and/or mechanical inadequacies (Fig. 3). The 2-block listric fault model could satisfactorily explain synthetic rollovers, especially if the involved extensional displacement is accommodated downslope by thrusting (Kehle, 1970; Mandl and Crans, 1981) (Fig. 3a). A direct natural example of this has been described in the Gulf of Mexico (see Fig. 10 in Peel et al., 1995) or offshore Australia (see Fig. 15 in Krassay and Totterdell, 2003). Conversely, in this 2-block listric fault model the development of antithetic rollovers is impossible for obvious dynamic reason (Fig. 3b) or kinematic compatibility (Fig. 3c). How could the upslope displacement of an antithetic rollover be accommodated by thrusting working against gravity (Fig. 3b)? How could synthetic and antithetic rollovers develop simultaneously in the same hangingwall block (Fig. 3c) without shortening in between them?

The above arguments show that the development of an antithetic rollover, rather common in salt tectonics, requires at least three blocks: i) an upslope block and a downslope block that move downslope at different rates above a basement block (Fig. 3d) or ii) a fixed upslope block that does not displace downslope but that simply rotates down the basement and a mobile downslope block (Fig. 3e). In the first case (Fig. 3d) the sense of shear below the rollover is opposite to the sense of shear along the master normal fault and in the second one (Fig. 3e) there is no shear at rollover base.

In these two configurations, the listric fault model (Fig. 2) cannot apply to the development of rollovers in terms of kinematic compatibility – i.e. senses of shear – (Fig. 3d) or absence of shear below the rollover (Fig. 3e). Consequently, the listric fault model (Fig. 2) that has been found useful for many years to describe some particular aspects of hangingwall deformation, does not properly explain the mechanics of rollovers in salt tectonics. However, analogue modelling experiments of gravity driven deformation of brittle–ductile models carried out in the past two decades (Vendeville and Cobbold, 1987; Vendeville et al., 1987; Cobbold and Szatmari, 1991; Vendeville and Jackson 1992a,b; Gaullier et al., 1993; Ge et al., 1997, Mauduit et al., 1997a,b; McClay et al., 1998; Mauduit, 1998; Mauduit and Brun, 1998; Brun and Fort, 2004; Fort et al., 2004a,b) contain an implicit but obvious solution to this problem.

On the basis of our analogue modelling results and their comparison with natural examples, we argue that the development of rollovers in salt tectonics is fundamentally nonsteady state and that it results from the mechanical instability of the sedimentary layers deposited on top a weak layer. From models, it is shown how synthetic and antithetic rollovers combine, into time and space, patterns directly comparable to natural examples. Finally, a simple 3-block model is used to discuss the four possible kinematics patterns for rollovers.

2. Modelling of rollovers

Two categories of analogue models are currently used in the laboratory to simulate the development of rollovers. The first category takes the listric shape of the fault as a boundary condition and studies the resulting deformation of the hangingwall. The second category defines, a brittle–ductile layered system subjected to gravity- and differential-load-driven deformation and studies in which circumstances rollovers develop in time, and space. We attempt here, a comparison of these two types of rollover modelling that differ not only in technical aspects but also in their conceptual bases, mechanical significance and practicable outcomes.

2.1. Steady state: the experimental listric fault model

The experimental setup is a direct laboratory application of the listric fault model (Fig. 2). A deformable hangingwall, made of a material able to fail under gravity forces – more generally sand or clay – is placed above a rigid footwall shaped to mimic a listric fault (Fig. 4). A “plastic sheet detachment” at the base of the hangingwall is pulled away from the fixed end-wall to simulate fault displacement. Synkinematic sedimentation is made at regular time intervals on top of the deforming hangingwall. Various experiments have been carried out to examine the effects of fault shape and dip on the hangingwall deformation and interactions between deformation and sedimentation (e.g. McClay and Ellis, 1987; Ellis and McClay, 1988; McClay 1990a, b; Dula, 1991; McClay and Scott, 1991; McClay, 1995).

In these experiments, the footwall is not deformable and there is no friction on the fault. As the fault shape does not change during experiment and as the materials used are not strain rate dependant, model deformation is steady state. Therefore, as long as displacement and sedimentation are maintained, the deformation regime does not change. Because there is no friction on the fault, deformation is only due to the downward flexure that the hangingwall undergoes when passing from the steep part to the flat part of the fault.

Most models produce spectacular rollover structures (Fig. 4b) with a prominent outer-arc extension accommodated by systems of Y-shape patterns of conjugate normal faults that define the so-called “keystone – or crestal collapsed – grabens”. The synkinematic layers display characteristic fan-like patterns with layer thickness increasing toward the fault. The angle α of obliquity between layers and the listric fault is constant as in the theoretical listric fault model (Fig. 2). The layer geometry does not show any shear drag against the fault, confirming the total lack of friction.

This type of model attempts only to explain the geometry and internal deformation of rollovers and not their regional setting, at whole basin scale, nor do they try to explain the origin of the rollover system or the way they evolve dynamically through time. It has already been shown that the application of the model to salt tectonics on passive margins (Fig. 3) leads to kinematical and/or mechanical inadequacies.

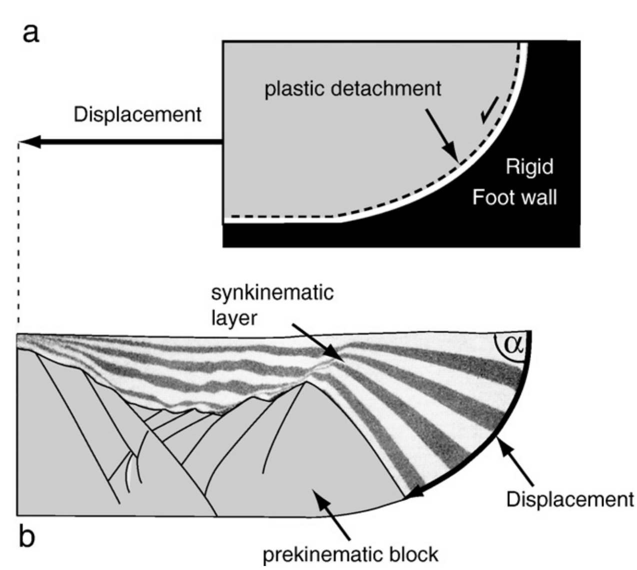

Fig. 4. Experimental rig used to simulate the growth and deformation of a rollover according to the listric fault model (a) and rollover model example (b). Modified after McClay et al. (1991).

2.2. Mechanical instability: the raft tectonics model

In this second category of rollover models, the sand–silicone technique designed to simulate the deformation of brittle–ductile systems (Faugère and Brun, 1984) is combined to synkinematic sedimentation to simulate the processes of salt tectonics (Vendeville and Cobbold, 1987). It provides a convenient experimental method to simulate in the laboratory the processes of “raft tectonics” that occur in basins deposited on top of weak layers, like salt (Burollet, 1975; Duval et al., 1992).

In the experiments presented in this paper, a two-layer sand–silicone model is placed on top of a rigid basal plate, where the upper brittle sand layer and the lower viscous silicone putty layer simulate overburden and salt, respectively. The basal plate is tilted allowing the model to spread downslope under its own weight. The strain rate is dependant on the viscosity of the silicone putty, the model thickness, the densities of sand and silicone putty and the basal slope angle (Mauduit et al., 1997b; Mauduit, 1998). As the model deforms, thin sand layers are deposited on model surface at regular time intervals to simulate synkinematic sedimentation. Because the downslope end of the model is a free boundary, the whole model undergoes extension. Synthetic normal faults dominate in the downslope domain. Both synthetic and antithetic faults commonly coexist in the upslope domain (Mauduit et al., 1997b). Deformation of the sand layer starts with small grabens, which generally evolve asymmetrically giving tilted blocks and/or growth faults and associated rollovers (Mauduit and Brun, 1998).

Fig. 5a and b illustrates two characteristic stages of development of synthetic rollovers. Fig. 6 shows two neighbouring rollovers associated with antithetic normal faults. In both synthetic and antithetic examples, a series of normal faults dipping opposite to the main growth fault or, a fan of conjugate normal faults, accommodates synkinematic layer bending. Comparable synthetic and antithetic rollover structures were obtained by other authors (e.g. see Fig. 4d in Vendeville and Cobbold, 1987; Fig. 3 in McClay et al., 1998). In Figs. 5 and 6, the basal silicone layer is made up of bars, square in section and perpendicular to the slope, of two alternating colours giving passive shear markers. Below both synthetic and antithetic rollovers, passive markers indicate a downslope sense of shear (see white arrows on Figs. 5 and 6). Therefore, in the antithetic case (Fig. 6), the senses of shear on the fault and in the ductile layer below the rollover are opposite, as already pointed out, on the basis of pure kinematic considerations (Fig. 3).

Such experiments produce a large variety of synthetic and antithetic rollover geometries, according to their stage of development that closely compares to the large variety of rollovers in nature (Fig. 1) (Mauduit and Brun, 1998). As illustrated in Figs. 5 and 6, such variety result from: i) irregular external rollover envelope, ii) various patterns of small faults inside the rollover, iii) layers shear drag against rollover external envelope and iv) different roller shapes.

Moreover, Mauduit and Brun (1998) (see in particular Figs. 5 and 6 and pp 18.123–18.124), have shown that a growth fault is mechanically unstable and that the growth of a single rollover is accommodated by successive transient active normal faults rather than by a single permanent one. In addition, the dip of the active fault changes during rollover growth leading to variations in the angle of obliquity α between layers and the rollover external envelope.

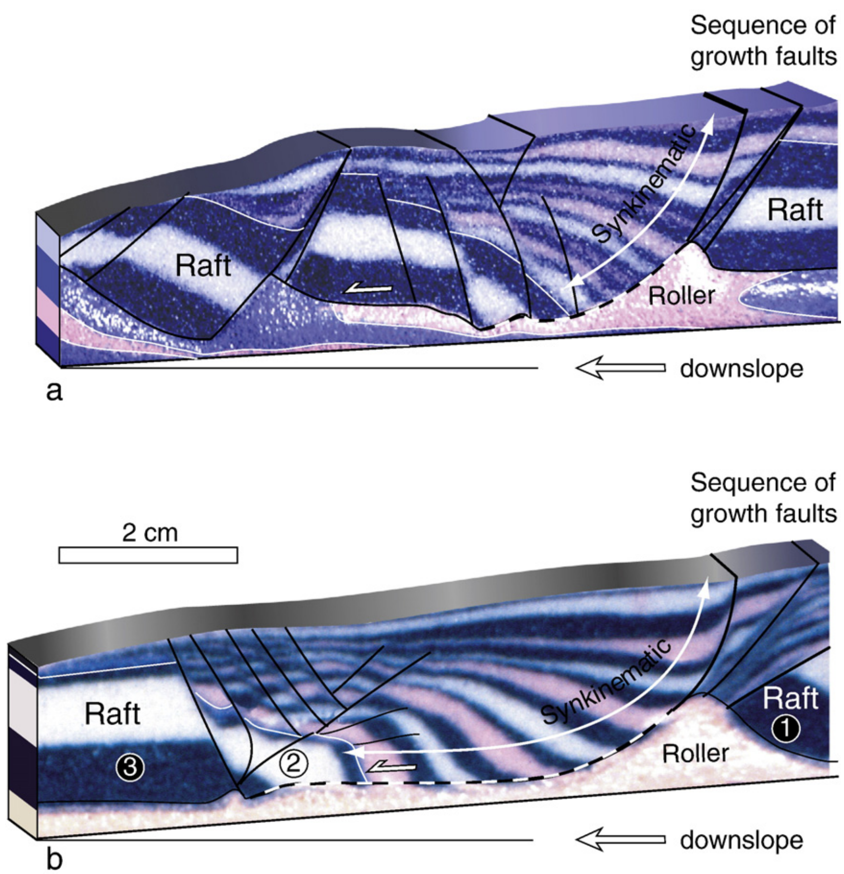

Fig. 5. Sections of synthetic rollovers obtained in gravity driven experiments on brittle–ductile models. The amount of displacement related to the rollover growth is smaller in (a) than in (b). The brittle layers are made of Fontainebleau sand with a frictional angle of 30° and the basal ductile layer is a Newtonian silicone putty (Rhodorsil© Gum GS1R, Rhone Poulenc) with a viscosity of 104 Pa s at room temperature. The thick “pre-kinematic” sand layer (from the silicone top to the white line) is deposited on top of the silicone layer before deformation. The thin “synkinematic” sand layers are deposited at regular time intervals during deformation. The silicone layer contains initially vertical coloured bands whose distortions indicate the sense of shear (white arrows). 1, 2 and 3 refer to the rafts of the pre-kinematic sand layer. The amount of displacement necessary to build the rollovers is 3 cm in (a) and 5 cm in (b). Note that the distortion of initially passive markers demonstrates the downslope sense of shear. (For interpretation of the references to colour in this figure legend, the reader is referred to the web version of this article.)

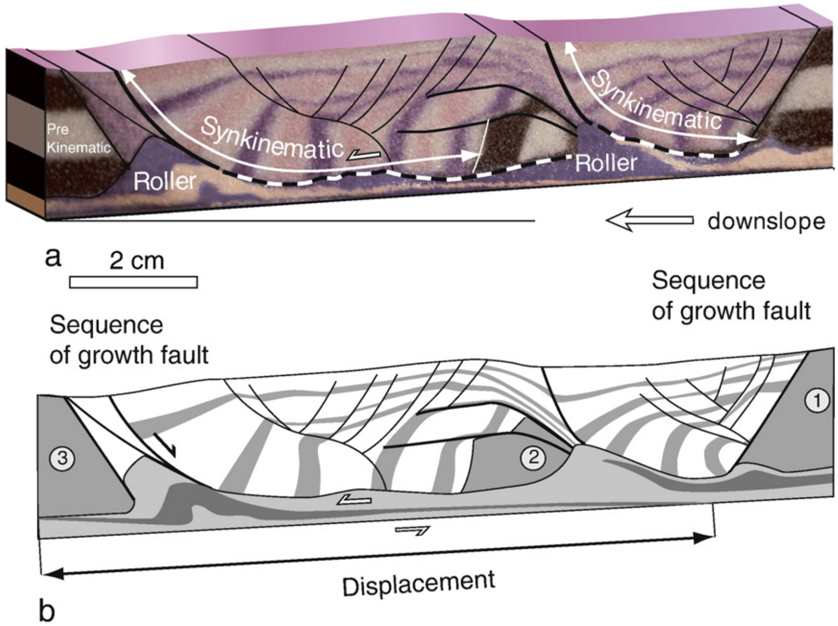

Fig. 6. Sections of an antithetic rollover (a) and line drawing (b). Experimental procedure and material properties are similar to those of Fig. 5. 1, 2 and 3 refer to the rafts of the pre-kinematic sand layer. Note that the sense of shear in the viscous layer is in kinematic contradiction with the sense of shear on the active normal fault that controls the rollover growth in the sand layer. The amount of displacement necessary to build the left hand rollover is 5.5 cm, and 3.5 cm for the right hand rollover. Note that the distortion of initially passive markers demonstrates the downslope sense of shear.

The three above experiments show that the development of a rollover in a brittle–ductile system is not a steady-state process. More generally, as portrayed in Fig. 7, extensional deformation starts in the brittle layer overlying the viscous layer, with initial grabens that further evolve toward a rollover. More commonly, deformation ends when the viscous layer almost disappears by thinning. Mauduit and Brun, (1998) have described the different possible modes of birth, growth and decays that can occur during the lifetime of growth fault rollover system. In summary, *in salt tectonics, the development of a rollover is not a steady-state process but, on the contrary, results from a mechanical instability with three main stages: birth, growth and decay* (Fig. 7). The ductile layer spreading corresponds to a layer-parallel simple shear combined to a pure shear — i.e. layer-parallel stretching and layer perpendicular shortening. The layer-parallel stretching is transmitted to the overlying brittle layer giving normal faulting and the formation of grabens within which rollovers further develop. This consists in the birth stage. On cross sections of largely extended models, rollovers developed between pre-kinematic rafts that formed initially graben shoulders (noted 1 and 3 in Figs. 5b and 6b). Rollovers therefore, grow on top of the initial graben inner block (noted 2 in Figs. 5b and 6b). The above features can be also identified in some seismic lines (e.g. Fig. 1b). The growth stage starts as soon as the inner block becomes tilted allowing the deposition of wedge shape sedimentary layers. During this growth stage, the ductile layer elongates with the rollover and therefore progressively thins. The decay stage is reached when the ductile layer thinning forbids further

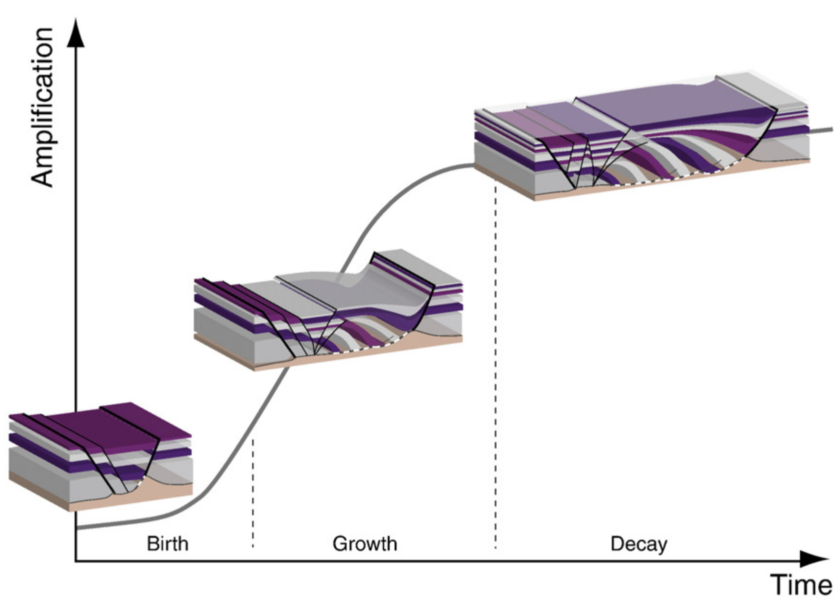

Fig. 7. Rollover evolution results from a mechanical instability with three main stages: birth, growth and decay (sketch modified after Mauduit and Brun, 1998, Fig. 9). The progressive thinning of the ductile layer will ultimately lead to the rollover-basement welding and then be responsible for the decay of the instability.

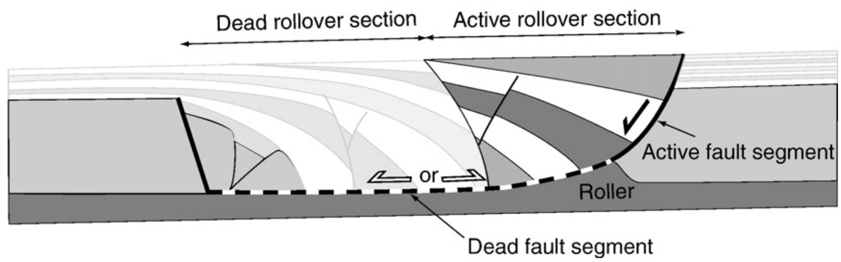

Fig. 8. Anatomy of a growing rollover. The main only active part of the rollover – shown in plain grey tones – corresponds to the domain bounded by the active growth fault, and a conjugate normal fault. See text for a full description.

rollover translation. The growth fault and the rollover are then passively covered by subsequent sedimentation (Fig. 7), as illustrated by the natural example of Fig. 1a.

The anatomy of a growing rollover presented in Fig. 8 summarises the above modelling results and their comparison with natural examples. The active part of the rollover is bounded by the main growth fault, on one side, and the conjugate small normal faults that accommodate layer bending, on the other side. The outer envelope of the rollover, despite its concave upward shape, cannot be considered as a listric fault. It is partly made of a frictional fault, in its steeply dipping upper part. Deeper, it corresponds to the hangingwall fault trace brought down into contact with the underlying décollement layer. The roller top represents the critical point at which the fault becomes inactive. The fault hangingwall made of the synkinematic layers undergo a downward rotation to become nearly horizontal. The amount of rotation of both the hangingwall block and synkinematic layers is therefore equal to the fault dip. The base of the rollover is then passively transported on top of the viscous layer. If the rollover is synthetic, the sense of transport is similar to the sense of shear on the frictional fault. On the contrary, if the rollover is antithetic the sense of transport is opposite. The base of the rollover acquires an upward concave shape whatever the sense of shear in the décollement layer. This points out that *the concave shape of a rollover base does not demonstrate that the corresponding growth fault has a listric shape*. It

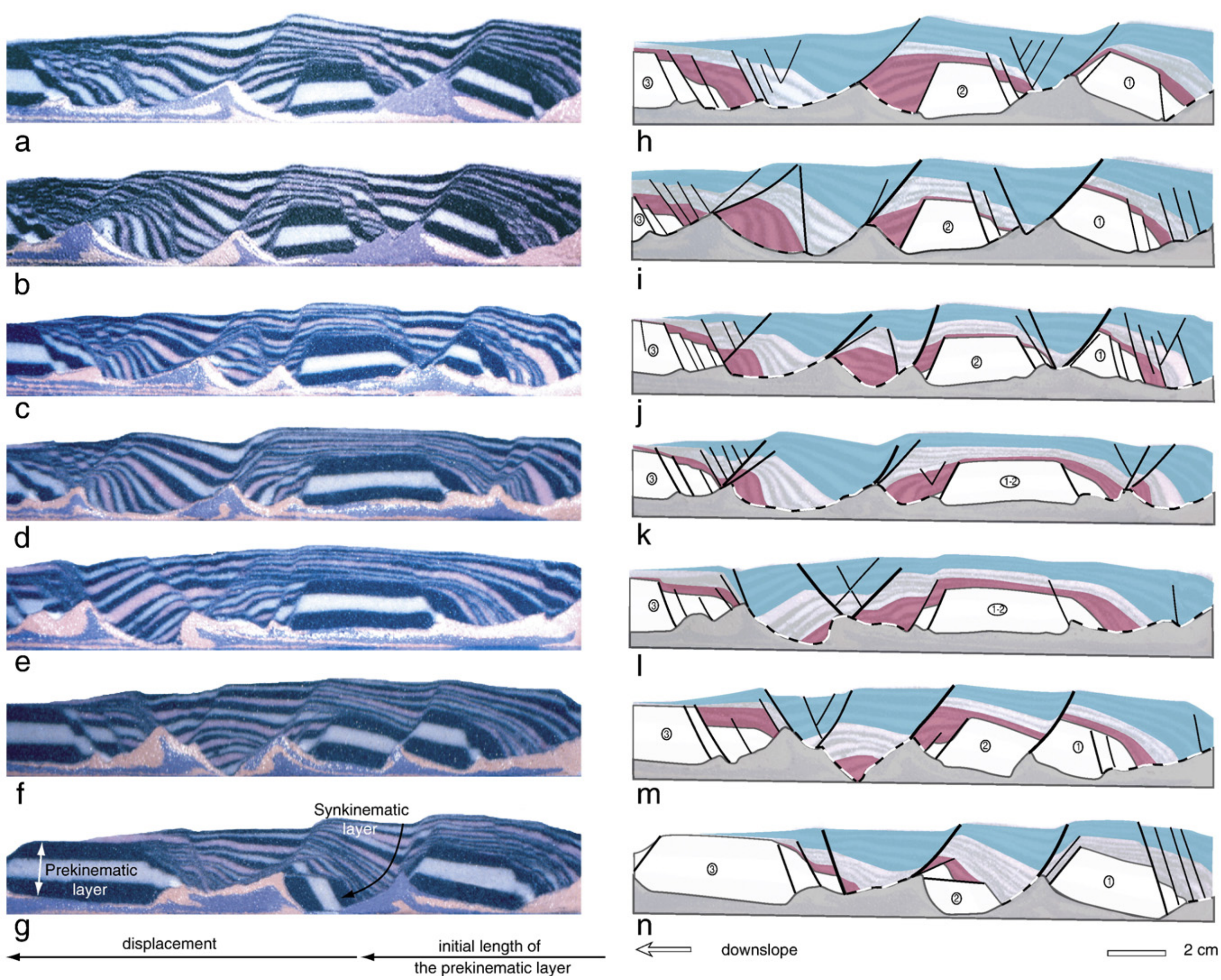

Fig. 9. Serial cross sections across the same model revealing complex 3D patterns of growth faults and associated rollovers (a to g), and structural interpretation (h to n). The 7 sections are cut parallel to the slope direction, and are 5 cm apart, i.e. the spacing between sections is roughly equal to the section height. The pre-kinematic sand layer as well as the viscous layer had a constant thickness of 2 cm. See text for description. The initial length of the undeformed section was 8.5 cm, and therefore the amount of displacement is 12 cm.

simply reflects the fact that a steeply dipping normal fault is connected to a flat lying décollement layer.

To summarise what precedes a growing rollover can be divided in two parts (Fig. 8): (1) an "active rollover section" bounded by the main growth normal fault, on one side, and a conjugate normal fault, on the other side, and (2) a "dead rollover section" not anymore submitted to deformation that is transported passively on top of the underlying ductile layer. Similarly, the external lower envelope of the rollover can be also divided in two parts: (1) an "active fault segment reaching the surface" that puts 2 sedimentary blocks into frictional contact and (2) a "dead fault segment" where the hangingwall block has been carried into contact with the underlying viscous décollement layer. It must be noted that a part of the dead fault segment is seated below the active rollover section.

3. Lateral variations of rollover asymmetry

Seismic surveys in domains of extensional salt tectonics often reveal complex 3D patterns of growth faults and associated rollovers. Such complexities are also commonly observed in laboratory experiments of gravity spreading–gliding on brittle–ductile models as exemplified by the serial sections shown in Fig. 9. In the central part of rollover domain (Fig. 9d–k and e–l) the pre-kinematic layer is cut into two main rafts, numbered 1–2 and 3, between which both synthetic (Fig. 9, d–k) and antithetic (Fig. 9, e–l) rollovers are located. Laterally, toward the lateral boundaries of the model, the raft 1–2 divides into sub-rafts 1 and 2.

The space between rafts 2 and 3 is dominantly occupied by a synthetic rollover from section a–h to section d–k, by an antithetic rollover in section e–l, by a nearly symmetrical graben in section f–m and finally, by a synthetic rollover in section g–n. Section d–k shows that an antithetic rollover has developed in the upslope block of the large synthetic rollover, at an early stage of deformation. Therefore, the transition between the synthetic and antithetic rollovers of sections d–k and e–l is not only a transition in space but also in time. The transition in space, from section d–k to section e–l, is progressive and does not involve any transform fault. Such progressive lateral transition between synthetic and antithetic rollovers excludes that both of them could be related to listric faults with opposite dips.

From sections e–l to f–m, the ductile layer has undergone a constant amount of stretching and a uniform sense of shear top to the left – i.e. downslope direction – between the pre-kinematic rafts 2 and 3. In contrast, this homogeneous pattern of ductile deformation in the décollement layer is accommodated by a variety of overlying synkinematic structures, including synthetic and antithetic rollovers. This demonstrates: i) that there is no simple kinematic relationship between the asymmetry of rollovers and the sense of shear in the underlying décollement and ii) that rollovers primarily represent the asymmetrical sedimentary infilling of opening grabens or separating rafts.

4. Discussion: rollover kinematics in salt tectonics

Based on the above theoretical considerations and experimental results, it appears that any kinematic model of rollovers, in salt tectonics, requires to consider three blocks. In the four kinematic configurations that can occur (Fig. 10), deformation in the upper brittle layer starts with the initiation of a graben that separates an upslope block from a downslope block in the upper brittle layer. The two blocks separate by rafting on top of the ductile décollement above the basement. In other words, this layer must be considered as a displacement zone between the 2 rafted blocks and the basement.

4.1. Synthetic rollovers

If the upslope block is not moving downslope – i.e. pinned to the basement – (Fig. 10a), displacement on the master normal fault is entirely transformed into ductile shear along the décollement layer below the downslope block and the growing rollover. Once deposited, new layers undergo friction along the fault until they come into contact with the ductile layer. Then, the fault trace is rotated to nearly horizontal and passively translated, parallel to the basement. Rotation of the hangingwall block and subsequent layer bending are accommodated by transient normal faults within the rollover. Progressive capping by synkinematic layer indicates a sequential development of these faults toward the main growth fault. The ductile material of the décollement layer can be extruded from below the upslope block into the roller to compensate thinning below the rollover.

If the upslope block is moving downslope (Fig. 10b), but at a rate lower than the downslope block, the amount of layer-parallel shear below the rollover results from the addition of the displacement accumulated on the master normal fault and of the one of the upslope block.

4.2. Antithetic rollovers

If the upslope block is pinned to the basement (Fig. 10c), the fault trace and the synkinematic layers are rotated downward on top of the ductile layer but not displaced downslope (see Fig. 3e). Therefore, contrary to the synthetic rollovers (Fig. 10a and b), the displacement on the master normal fault is not transformed into ductile shear along the décollement layer below the growing rollover. It is only below the downslope block that the décollement layer undergoes layer-parallel shear. Ductile material of the décollement layer is extruded downward from below the upslope block and the growing rollover. This model where the rollover does not move with respect to the basement partially meets the experimental models of prograding delta (Ge et al., 1997; McClay et al., 1998). It could possibly apply to the large-scale antithetic rollover of the Brazilian margin (Fig. 1f) (Demercian et al., 1993) if it can be proven that no extension occurs in the upslope part of the margin. If the upslope block is not pinned, (Fig. 10d) the rollover moves downslope and the underlying ductile layer is sheared in a sense opposite to the sense of shear on the master fault. This is observed in many experimental models of antithetic rollover (e.g. Fig. 6), and more likely applies to natural examples such as those of Fig. 1c and e. It would also apply to the example of the Brazilian margin (Fig. 1f), if extension exists in the upslope part of the margin.

4.3. The role of the ductile layer

Two decades of laboratory experiments on brittle–ductile models (Vendeville and Cobbold, 1987; Vendeville et al., 1987; Mauduit et al., 1997b; Mauduit and Brun, 1998; Fort et al., 2004a,b; Brun and Fort, 2004) have greatly contributed to the understanding of the mechanics and kinematics ruling the most widespread structures encountered in gravity driven deformation. It is because ductile layers react to even minor differential stresses, like those created by basement tilting and/or differential sedimentary loading, that salt tectonics gives birth to a large variety of syn-sedimentary structures, both in extensional and contractional regimes. The brittle–ductile models presented in the current contribution (Figs. 5, 6 and 9), and the geometrical and kinematical rules deduced from their study (Fig. 10), emphasise the paramount role of ductile layers, in particular salt layers, in the development of rollovers as a mechanical instability (Fig. 7).

At the onset of gravity driven deformation, a thick ductile layer strongly decouples the sedimentary cover from the basement and leads to the development of grabens. A thinner ductile layer increases the coupling between the cover and the basement and tilted blocks develop instead of grabens (see Mauduit et al., 1997b; Fort et al., 2004a for a detailed analysis). With increasing extension and rollover growth the ductile layer is submitted to a combination of simple shear and pure shear (Mauduit et al., 1997b). The simple shear component results from layer-parallel displacement due to sliding–spreading on top of the basement. The pure shear component results from a ductile layer thinning proportional to the rollover lengthening. Ultimately, the ductile layer thickness can undergo extreme thinning leading to a rollover-basement welding (Fig. 1a). This is likely the most common reason for rollover decay (Fig. 7) (Mauduit and Brun, 1998).

4.4. Kinematic rules

In all configurations, except the antithetic rollover with a fixed upslope block, kinematics has the following characters (Fig. 10a, b and d):

(1) The sense of layer-parallel shear, below both synthetic and antithetic rollovers, is always directed top to downslope.
(2) The intensity of layer-parallel shear, shown in Fig. 10 by the distortion of the initially vertical markers, is controlled below synthetic rollovers by the displacement accumulated on the master normal fault and the amount of upslope block displacement (Fig. 10a and b). Below antithetic rollovers, the ductile layer is extruded downslope under the upslope block and the rollover and is sheared top downslope below the downslope block (Fig. 10c and d).
(3) The thinning of the décollement layer below a rollover directly depends on the amount of separation between the upslope and downslope blocks. In other words, the thinning of the décollement layer is a direct function of the rollover size.

This three-block kinematic model implies that an isolated rollover has no general kinematic significance with respect to the underlying basement. It is noteworthy that, for antithetic growth faults, the

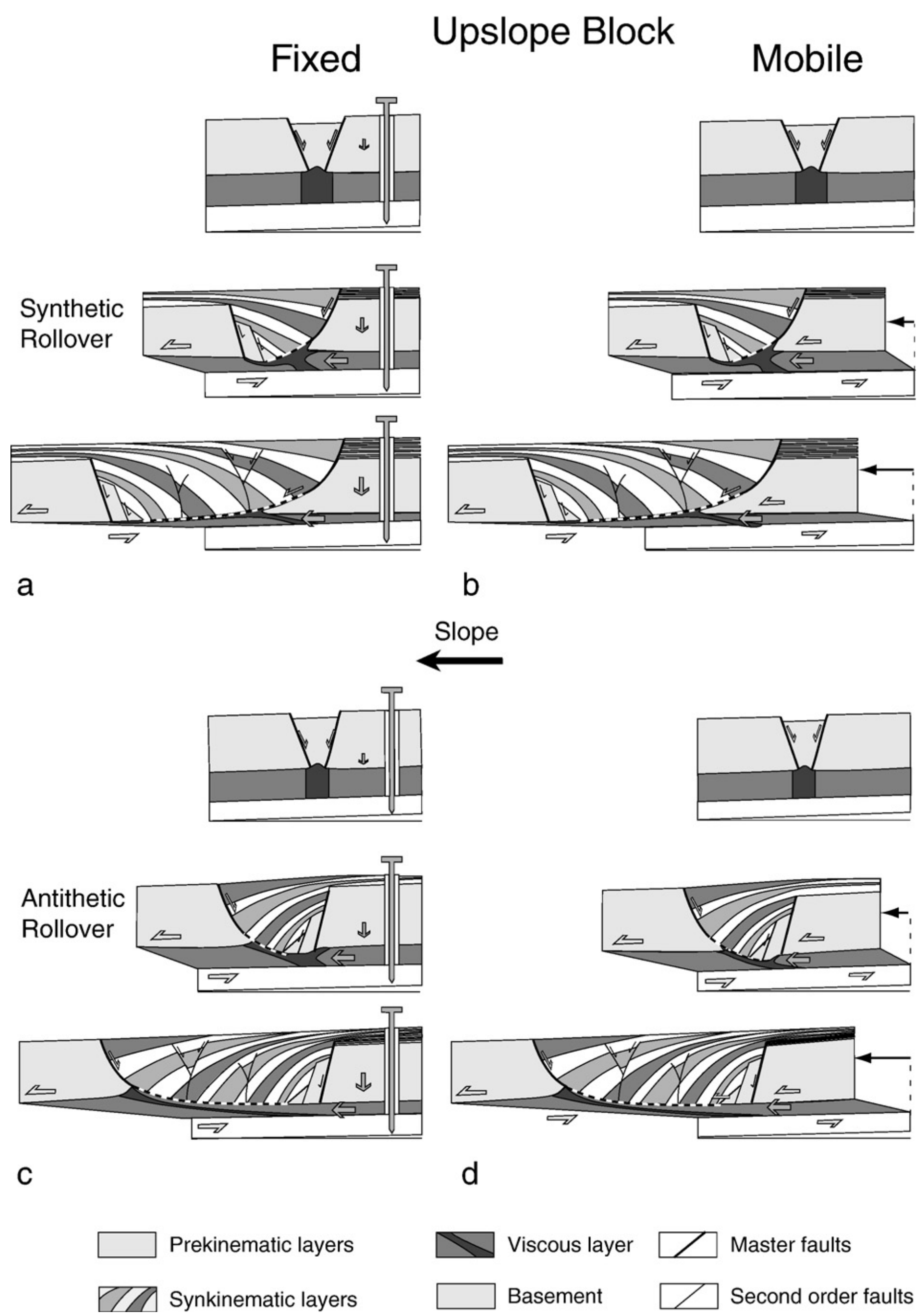

Fig. 10. Four kinematics configuration possible for rollovers development. a and b, Synthetic rollovers, c and d antithetic rollovers. Note that the sense of shear in the viscous layer is always directed top downslope. The intensity of layer-parallel shear, shown by the distortion of the initially vertical markers, is controlled below synthetic rollovers (a and b) by the displacement accumulated on the master normal fault and the amount of upslope block displacement. In the case of antithetic rollovers (c and d), the ductile layers is extruded downslope under the upslope block and the rollover and is sheared top downslope below the downslope block. Compare with the distortion of the initially passive markers in the silicone layers of experiment shown in Figs. 5 and 6.

sense of shear along the flat lying base of the rollover can be opposite to the sense of shear along the fault. A rollover structure only records the separation between two neighbouring blocks moving above a low angle décollement. A given isolated rollover may correspond to four kinematic configurations (Fig. 10). Only an analysis on the scale of the whole thin-skin extensional system can discriminate between them.

5. Conclusions

Examination of numerous seismic examples, theoretical considerations and analogue modelling leads us to conclude that the "listric fault model" is inadequate to explain the origin of rollovers in salt tectonics. According to this model, a rollover growth is steady state, by nature, and related to the relative displacement of two blocks.

In contrast, the development of a rollover in salt tectonics is not steady state and requires a three-block system:

(1) Rollover growth results from a mechanical instability defining a critical lifetime with three characteristic stages: birth, growth, and decay.
(2) The rollover is located between an upslope block and a downslope block that separate from each other on top of a décollement layer above an underlying basement block.
(3) The rollover can be either synthetic or antithetic with reference to the large-scale kinematics of the extensional system.

The characteristic anatomy of a growing rollover is defined by:

(4) A fan-like pattern of synkinematic layers that result from the interaction between a steeply dipping normal fault and an extending ductile layer, underneath.
(5) A concave upward external envelope made of a steeply dipping active normal fault, in the upper part, and of the hangingwall fault trace brought down into contact with the underlying décollement layer. This upward concave shape is acquired whatsoever the sense of shear in the salt layer. This points out that the concave shape of the rollover base is not an argument in favour of listric faulting.
(6) Small normal faults dipping parallel to and/or toward the master normal fault that accommodate the bending of synkinematic layers inside the rollover and that develop in sequence toward the master normal fault.
(7) The presence of a ductile roller at the base of the active master normal fault.

From a kinematic point of view, except in the case of antithetic rollovers whose upslope block is fixed, synthetic rollovers as well as antithetic rollovers move downslope above the underlying décollement layer. This explains that synthetic and antithetic rollovers can pass laterally to each other without transform fault or can follow each other in the direction of displacement to give turtle back-type structures. If it can be stated that the listric shape of a fault is responsible for the rollover folding of the hangingwall, the reverse is not true. As argued in details, in this paper, in salt tectonics, a rollover does not imply the existence of a listric fault.

Acknowledgements

We have been trying to convey the ideas reflected in this paper for many years. We have had therefore, plenty of opportunities to talk about this particular issue with a number of colleagues that we have not necessarily convinced… The listric fault model dies hard! Nevertheless, we are indebted to all of them among whom, are in particular K.R. McClay, B.C. Vendeville, M.O. Withjack and our colleagues and friends from Rennes and Amsterdam P.R. Cobbold, X. Fort and D. Sokoutis. We would also like to acknowledge collaborations with Norsk Hydro, Shell and Total (Elf) without which we would have never carried out this work. We are greatly indebted to issues made by T. Dooley and an anonymous referee that considerably helped in improving the manuscript.

References

Bally, A.W., 1981. Thoughts on the tectonics of folded belts. In: Mc Clay, K.R., Price, N.J. (Eds.), Thrust and Nappes Tectonics. Geol. Soc. London Spec. Publ., vol. 9, pp. 13–32.
Bally, A.W., Bernouilli, D., Davis, G.A., Montadert, L., 1981. Listric normal faults. Oceanol. Acta 87–101 N° SP.
Bhattacharya, J.P., Davies, R.K., 2001. Growth faults at the prodelta to delta front transition, Cretaceous Ferron sandstone. Utah Mar. Petrol. Geol. 18, 525–534.
Bradshaw, G.A., Zoback, M.D., 1988. Listric normal faulting, stress refraction, and the state of stress in the Gulf Coast basin. Geology 16, 271–274.
Braun, J., Batt, G.E., Scott, D.L., McQueen, H., Beasley, A.R., 1994. A simple kinematic model for crustal deformation along two- and three-dimensional listric normal faults derived from scaled laboratory experiments. J. Struct. Geol. 16, 1477–1490.
Broucke, O., Temple, F., Rouby, D., Robin, C., Calassou, S., Nalpas, T., Guillocheau, F., 2004. The role of deformation processes on the geometry of mud-dominated turbiditic systems, Oligocene and Lower-Middle Miocene of the Lower Congo basin (West African Margin). Mar. Pet. Geol. 21, 327–348.
Bruce, C.H., 1973. Pressured shale and related sediment deformation: mechanism for development of regional contemporaneous faults. Am. Assoc. Pet. Geol. Bull. 57, 878–886.
Brun, J.-P., Fort, X., 2004. Compressional salt tectonics (Angolan Margin). Tectonophysics 382, 129–150.
Burollet, P.F., 1975. Tectonique en radeaux en Angola. Bull. Soc. Géol. Fr. 17, 503–504.
Cloos, E., 1968. Experimental analysis of Gulf Coast fracture patterns. Am. Assoc. Pet. Geol. Bull. 52, 420–444.
Cobbold, P.R., Szatmari, P., 1991. Radial gravitational gliding on passive margins. Tectonophysics 188, 249–289.
Davison, I., 1986. Listric normal fault profiles, calculation using bed-length balance and fault displacement. J. Struct. Geol. 8, 209–210.
Demercian, S., Szatzmari, P., Cobbold, P.R., 1993. Style and pattern of salt diapirs due to thin-skinned gravitational gliding, Campos and Santos basins. Offshore Brazil. Tectonophysics 228, 393–433.
Dula, W.F., 1991. Geometric models of listric normal faults and rollovers folds. Am. Assoc. Pet. Geol. Bull. 75, 1609–1625.
Duval, B., Cramez, C., Jackson, M.P.A., 1992. Raft tectonics in the Kwanza (Cuenza) Basin, Angola. Mar. Pet. Geol. 9, 389–404.
Doust, H., Omatsola, E., 1990. Niger Delta. In: Edwards, J.D., Santogrossi, P.A. (Eds.), Divergent/Passive Margin Basins. Am. Assoc. Pet. Geol. Mem., vol. 48, pp. 201–238.
Edwards, M.B., 1976. Growth faults in upper Triassic deltaic sediments, Swalbard. Am. Assoc. Pet. Geol. Bull. 60, 341–355.
Ellis, P.G., McClay, K.R., 1988. Listric extensional fault systems. Results of analogue model experiments. Basin Res. 1, 55–70.
Faugère, E., Brun, J.-P., 1984. Modélisation expérimentale de la distension continentale. C. R. Acad. Sci., Paris 299, 365–370.
Faure, J.L., Chermette, J.C., 1989. Deformation of tilted blocks, consequences on block geometry and extension measurements. Bull. Soc. Geol. Fr. 12, 461–476.
Fort, X., Brun, J.-P., Chauvel, F., 2004a. Salt tectonics on the Angolan margin, synsedimentary deformation processes. Am. Assoc. Pet. Geol. Bull. 88, 1523–1544.
Fort, X., Brun, J.-P., Chauvel, F., 2004b. Contraction induced by block rotation above salt. Mar. Pet. Geol. 21, 1281–1294.
Gaullier, V., Brun, J.-P., Guerin, G., Lecanu, H., 1993. Raft tectonics: the effect of residual topography below a salt decollement. Tectonophysics 228, 363–381.
Ge, H., Jackson, M.P.A., Vendeville, B.C., 1997. Kinematics and dynamics of salt tectonics driven by progradation. Am. Assoc. Pet. Geol. Bull. 81, 398–423.
Gibbs, A.D., 1983. Balanced cross section construction from seismic sections in areas of extensional tectonics. J. Struct. Geol. 5, 153–160.
Gibbs, A.D., 1984. Structural evolution of extensional basin margins. J. Geol. Soc. (Lond.) 141, 609–620.
Gibbs, A.D., 1985. Discussion on the structural evolution of extensional basin margins. J. Geol. Soc. (Lond.) 142, 939–942.
Hauge, T.A., Gray, G.G., 1996. A critique of techniques for modelling normal-fault and rollover geometries. In: Buchanan, P.G., Nieuwland, D.A. (Eds.), Modern Developments in Structural Interpretation, Validation and Modelling. Geol. Soc. Spec. Publ., vol. 99, pp. 89–97.
Imber, J., Childs, C., Nell, P.A.R., Walsh, J.J., Hodgetts, D., Flint, S., 2003. Hanging wall fault kinematics and footwall collapse in listric growth fault systems. J. Struct. Geol. 25, 197–208.
Kehle, R.O., 1970. Analysis of gravity sliding and orogenic translation. Geol. Soc. Amer. Bull. 81, 1641–1664.
Kerr, H.G., White, N., 1992. Laboratory testing of an automatic method for determining normal fault geometry at depth. J. Struct. Geol. 14, 873–885.
Krassay, A., Totterdell, J., 2003. Seismic stratigraphy of a large, Cretaceous shelf-margin delta complex, offshore Southern Australia. Am. Assoc. Pet. Geol. Bull. 87 (6), 935–963.
Liro, L.M., Coen, R., 1995. Salt deformation history and postsalt structural trends, offshore southern Gabon, West Africa. In: Jackson, M.P.A., Roberts, D.G., Snelson, S. (Eds.), Salt Tectonics, a Global Perspective. Am. Assoc. Pet. Geol. Mem., vol. 65, pp. 323–331.
Lundin, E.L., 1992. Thin skin extensional tectonics on a salt detachment, Northern Kwanza Basin, Angola. Mar. Pet. Geol. 9, 405–411.
Mandl, G., Crans, W., 1981. Gravitational gliding in deltas. In: McClay, K.C., Price, N.J. (Eds.), Thrust and Nappes Tectonics. Geol. Soc. London Spec. Publ., vol. 9, pp. 41–54.

Mauduit, T., 1998. Déformation Gravitaire Synsédimentaire sur une Marge Passive. Modélisation Analogique et Application au Golf de Guinée. Mém. Géosci. Rennes, 83. Géosciences Rennes, France.
Mauduit, T., Brun, J.-P., 1998. Development of growth fault/rollover systems. J. Geophys. Res. 103, 18,119–18,130.
Mauduit, T., Gaullier, V., Guérin, G., Brun, J.-P., 1997a. On the asymmetry of turtle back growth anticlines. Mar. Pet. Geol. 14, 763–771.
Mauduit, T., Guérin, G., Brun, J.-P., Lecanu, H., 1997b. Raft tectonics, the effects of basal slope value and sedimentation rate on progressive deformation. J. Struct. Geol. 19, 1219–1230.
McClay, K.R., 1990a. Physical models of structural styles during extension. In: Tankard, A.J., Balkwill, H.R. (Eds.), Extensional Tectonics of the North Atlantic margin. Am. Assoc. Pet. Geol. Mem., vol. 46, pp. 95–110.
McClay, K.R., 1990b. Extensional fault systems in sedimentary basins: a review of analogue models studies. Mar. Pet. Geol. 7, 206–233.
McClay, K.R., 1995. 2D and 3D analogue modelling of extensional fault structures, templates for seismic interpretation. Pet. Geosci. 1, 163–178.
McClay, K.R., 1996. Recent advances in analogue modeling, uses in section interpretation and validation. In: Buchanan, P.G., Nieuwland, D.A. (Eds.), Modern Developments in Structural Interpretation, Validation and Modelling. Geol. Soc. Lond. Spec. Publ., vol. 99, pp. 201–205.
McClay, K.R., Ellis, P.G., 1987. Analogue models of extensional fault geometries. In: Coward, M.P., Dewey, J.F., Hancock, P.L. (Eds.), Continental Extensional Tectonics. Geol. Soc. Lond. Spec. Publ., vol. 28, pp. 109–125.
McClay, K.R., Scott, A.D., 1991. Experimental models of hangingwall deformation in rampflat listric extensional fault systems. Tectonophysics 188, 85–96.
McClay, K.R., Waltham, D.A., Scott, A.D., Abousetta, A., 1991. Physical and seismic modeling of listric fault geometries. In: Tankard, A.J., Balkwill, H.R. (Eds.), The Geometry of Normal Faults. Geol. Soc. Spec. Publ., vol. 56, pp. 231–239.
McClay, K.R., Dooley, T., Lewis, G., 1998. Analog modeling of progradational delta systems. Geology 26, 771–774.
Mohriak, W.U., Macedo, J.M., Castellani, R.T., Rangel, H.D., Barros, A.Z.N., Latgé, M.A., Ricci, J.A., Mizusaki, A.M., Szatmari, P., Demercian, L.S., Rizzo, J.G., Aires, J.R., 1995. Salt tectonics and structural styles in the deep water province of the Cabo Frio Region, Rio de Janeiro, Brazil. In: Jackson, M.P.A., Roberts, D.G., Snelson, S. (Eds.), Salt Tectonics, a Global Perspective. Am. Assoc. Pet. Geol. Mem., vol. 65, pp. 305–321.
Nelson, T.H., 1991. Salt tectonics and listric normal faulting. In: Salvador, A. (Ed.), The Gulf of Mexico Basin. Geol. Soc. Amer., Boulder, Colorado, pp. 73–89.
Peel, F.J., Travis, C.J., Hossack, J.R., 1995. Genetic structural provinces and salt tectonics of the Cenozoic offshore U.S. Gulf of Mexico: a preliminary analysis. In: Jackson, M.P.A., Roberts, D.G., Snelson, S. (Eds.), Salt Tectonics: a Global Perspective. AAPG Mem., vol. 65, pp. 153–175.
Poblet, J., Bulnes, M., 2005. Fault-slip, bed-length and area variations in experimental rollover anticlines over listric normal faults: influence in extension depth to detachment estimations. Tectonophysics 396, 97–117.
Price, N.J., 1977. Aspect of gravity tectonics and the development of listric faults. J. Geol. Soc. (Lond.) 133, 311–327.
Rider, M.H., 1978. Growth faults in carboniferous of Western Ireland. Am. Assoc. Pet. Geol. Bull. 62, 2191–2213.
Rouby, D., Raillard, S., Guillocheau, F., Bouroullec, R., Nalpas, T., 2002. Kinematics of a growth fault/raft system on the West African margin using 3D restoration. J. Struct. Geol. 24, 783–796.
Seranne, M., Seguret, M., Fauchier, M., 1992. Seismic super-units and post rift evolution of the continental passive margin of southern Gabon. Bull. Soc. Geol. Fr. 163, 135–146.
Shelton, J.W., 1984. Listric normal fault, an illustrated summary. Am. Assoc. Pet. Geol. Bull. 68, 801–815.
Szatmari, P., Guerra, M.C.M., Pequeno, M.A., 1996. Genesis of large counter regional fault by flow of Cretaceous Salt in the South Atlantic Santos Basin, Brazil. In: Alsop, G.I., Blundell, D.J., Davison, I. (Eds.), Salt Tectonics. Geol. Soc. Spec. Pub., vol. 100, pp. 259–264.
Vendeville, B., 1991. Mechanisms generating normal fault curvature: a review illustrated by physical models. In: Roberts, A.M., Yielding, G., Freeman, B. (Eds.), Geol. Soc. Spec. Pub., vol. 56, pp. 241–249.
Vendeville, B., Cobbold, P.R., 1987. Glissements gravitaires synsédimentaires et failles normales listriques, modèles expérimentaux. C. R. Acad. Sci. 305 (II), 1313–1319.
Vendeville, B., Jackson, M.P.A., 1992a. The rise of diapirs during thin skinned extension. Mar. Pet. Geol. 9, 331–353.
Vendeville, B., Jackson, M.P.A., 1992b. The fall of diapirs during thin skinned extension. Mar. Pet. Geol. 9, 354–371.
Vendeville, B., Cobbold, P.R., Davy, P., Brun, J.P., Choukroune, P., 1987. Physical models of extensional tectonics at various scales. In: Coward, M.P., Dewey, J.F., Hancock, P.L. (Eds.), Continental Extensional Tectonics. Geol. Soc. Lond. Spec. Pub., vol. 28, pp. 95–107.
Wheeler, J., 1987. Variable-heave models of deformation above listric normal faults: the importance of area conservation. J. Struct. Geol. 9, 1047–1049.
White, N., Jackson, J.A., McKenzie, D.P., 1986. The relationships between the geometry of normal faults and that of the sedimentary layers in their hanging walls. J. Struct. Geol. 8, 897–909.
William, G., Vann, I., 1987. The geometry of listric normal faults and deformation in their hangingwalls. J. Struct. Geol. 9, 789–795.
Withjack, M.O., Peterson, E., 1993. Prediction of normal fault geometries. A sensitivity analysis. Am. Assoc. Pet. Geol. Bull. 77, 1860–1873.
Xiao, H.B., Suppe, J., 1989. Origin of rollover. Am. Assoc. Pet. Geol. Bull. 76, 509–529.